THE BELL SYSTEM TECHNICAL JOURNAL
Vol. 58, No. 3, March 1979
Printed in U.S.A.

Determination of the Basic Device Parameters of a GaAs MESFET

By H. FUKUI

(Manuscript received July 28, 1978)

This paper describes a new technique to determine the basic properties of the active channel of a gallium arsenide (GaAs) metal-semiconductor field effect transistor (MESFET). The effective gate length, channel thickness, and carrier concentration are determined from dc parameters. A precise method of measuring the dc parameters is also given. The new techniques are demonstrated using a wide variety of sample devices. It is also shown that microwave performance parameters, such as the maximum output power and minimum noise figure, are well predicted by dc parameters. Calculated values of the intrinsic and extrinsic dc parameters, using simple analytical expressions developed in terms of the geometrical and material parameters of a device, are shown to be in excellent agreement with their measured values. These expressions can be used as a basis for device design.

I. INTRODUCTION

In a gallium arsenide (GaAs) metal-semiconductor field effect transistor (MESFET), the properties of the active channel are fundamental in describing its operation. The channel properties can be characterized by the four basic parameters: gate length, gate width, channel thickness, and channel doping.

In a recent paper,[1] the maximally obtainable value of channel current was defined as the maximum channel current, I_m. It was pointed out that I_m differs from either (fully open channel) saturation current, I_s, or zero-gate-bias drain current, which is often referred to as I_{dss}. Currents I_s and I_{dss} have conventionally been used to show upper limits of the drain current capability. However, neither I_s nor I_{dss} can represent the maximally obtainable value of channel current. It was emphasized that I_m plays an important role in determining the maximum capability of large-signal operation of the device. Simple expres-

sions for I_m were then obtained in terms of the four basic channel parameters, as a result of an extended study of Shockley's gradual channel approximation[2] on Grebene-Ghandhi's two-section FET model[3] with Fukui's concept on the current limiting mechanism.[1]

Among the four basic channel parameters, the total gate width, Z, is usually a given factor or merely a scaling factor. Therefore, the other three parameters are noted to be the most crucial variables in the design work. For these three parameters, their effective values were adopted in Ref. 1. This was essential, especially for gate length. The effective gate length, L, may be either shorter or longer than the physical length of gate metallization, L_g, depending upon the gate junction topography. The channel thickness, a, and carrier concentration, N, represent their effective values in the active region of the channel.

In Ref. 1, practical expressions for the zero-gate-bias channel current, I_o, were also developed as functions of the basic channel parameters N, a, L, and Z, and an additional parasitic parameter of source series resistance, R_s. An approximate expression for the knee voltage, V_{kf}, corresponding to I_m in the drain I-V characteristic, was given by a combination of N, a, L, Z, R_s, and R_d on a semi-empirical basis, R_d being the drain series resistance. In addition, it has been known that the total pinch-off voltage, W_p, is determined by the Na^2 product and that W_p is equal to the sum of terminal pinch-off voltage, V_p, and Schottky-barrier built-in voltage, V_b.

It is now conceivable that N, a, and L may be determined from the measured values of I_m, I_o, V_{kf}, V_p, V_b, R_s, and R_d, provided that Z is known. The prime purpose of this paper is to present a new technique for carrying out this work. Throughout the paper, a transistor curve tracer is exclusively used as the tool necessary for measuring the dc parameters. However, test equipment of other types with the equivalent functions can, of course, be used as well.

There has been a common practice in which either a or N is determined from V_p, after knowing either N or a, respectively, and assuming an appropriate value of V_b. Also, Fair showed that an iterative analysis on I_o, R_s, and transconductance, g_m, makes it possible to determine N and a from known values of I_o, V_p, and terminal transconductance, g'_m.[4] However, as far as the author knows, there has been no published report on an evaluation technique for the effective gate length of a finished device. This paper presents such a technique as well as simultaneous determination of N and a, from known values of I_m, I_o, V_p, V_b, V_{kf}, R_s, and R_d.

The second purpose of this paper is to show prediction of the microwave performance parameters, such as the maximum output power and minimum noise figure, from the dc parameters and hence the basic channel parameters. To predict the minimum noise figure,

the values of g_m and R_g, which is the gate series resistance, must be known. Therefore, the determination of g_m and R_g are also described in this paper. Once the detail of the structure outside the gate channel is given, the parasitic parameters, such as R_g, R_s, and R_d, can be analytically expressed in terms of the geometrical and material parameters of the corresponding sections of the device. The validity of such expressions is then examined with experimental results in this paper.

II. PRINCIPLE OF NEW TECHNIQUE

2.1 Analytical expressions for device dc parameters

To determine the basic channel parameters of a GaAs MESFET from the measured values of its dc parameters, expressions showing their relationships are essential. It has been well known that W_p and I_s are given by

$$W_p = \frac{qNa^2}{2\kappa\epsilon_0} \tag{1}$$

and

$$I_s = qv_sNaZ, \tag{2}$$

respectively,[5] in which q is the electronic charge, ϵ_0 is the permittivity of free space, κ is the specific dielectric constant, and v_s is the saturated velocity of electrons in n-GaAs. Substituting $q = 1.60 \times 10^{-19}$ C, $\epsilon_0 = 8.85 \times 10^{-14}$ F/cm, $\kappa = 12.5$ for GaAs, and a best fit value of $v_s = 1.4 \times 10^7$ cm/sec (Ref. 1) into (1) and (2) yields the following practical expressions:

$$W_p = 7.23Na^2 = V_p + V_b \quad \text{(V)} \tag{3}$$

and

$$I_s = 0.224ZNa \quad \text{(A)}, \tag{4}$$

where N is in units of 10^{16} cm^{-3}, a is in μm, and Z is in mm.

As mentioned earlier, analytical expressions for I_m, I_o and V_{kf} have been derived in Ref. 1. First, an expression for I_m is given in the form

$$I_m = \beta I_s, \tag{5}$$

where β is the maximum channel opening factor. Parameter β is expressed approximately as

$$\beta \approx 1 - \frac{0.18}{a}\sqrt{\frac{L}{N}} \tag{6}$$

provided that a best-fit value of 0.29×10^4 V/cm is assumed for the critical electric field, E_c. Another approximate expression for I_m is shown as

$$\frac{I_m}{Z} \approx \frac{0.18 N^{1.3} a^{1.5}}{L^{0.28}} \quad \text{(A/mm)}. \tag{7}$$

Second, an expression for I_o is given in the form

$$I_o = \gamma I_s, \tag{8}$$

where

$$\gamma \approx 1 + \sigma - \sqrt{\delta + 2\sigma + \sigma^2} \tag{9}$$

$$\delta = \frac{V_b + 0.234L}{W_p} \tag{10}$$

and

$$\sigma = \frac{0.0155 R_s Z}{a}. \tag{11}$$

Another approximate expression for γ is given by

$$\gamma \approx \left[1 - \frac{1}{\sqrt{W_p'}}\right]\left[1 - \frac{I_s R_s}{2\sqrt{W_p'}}\right], \tag{12}$$

where

$$W_p' = W_p + V_c. \tag{13}$$

In (13), V_c is a correction voltage that may vary from zero to a few tenths of a volt, depending upon the configuration of the channel structure. No analytical form is presently available for V_c.

Third, an expression for V_{kf} is given by

$$V_{kf} \approx (1 - \beta)^2 W_p + I_f(R_s + R_d) + V_c, \tag{14}$$

where I_f is the maximum value of total forward drain current, including the leakage current through the buffer layer and substrate.

2.2 Determination of basic channel parameters: Case I

If any one of the basic channel parameters N, a, and L is known, the other two can be determined from known values of V_p, V_b, and (I_m/Z) in a straightforward manner, using either a set of (3), (4), (5), and (6), or (3) and (7). For example, if the N value is known as a result of the epitaxial layer evaluation, a is readily determined by

$$a = \sqrt{\frac{V_p + V_b}{7.23N}} \quad (\mu\text{m}), \tag{15}$$

as is well known. The maximum channel opening factor is evaluated as

$$\beta = \frac{12 I_m/Z}{\sqrt{N(V_p + V_b)}}. \tag{16}$$

Using this β value, L is determined by

$$L = 4.27(V_p + V_b)(1 - \beta)^2 \quad (\mu\text{m}). \tag{17}$$

In the case that L (or a) is known, similar evaluation for N and a (or N and L) can also be carried out as well.

Among dc parameters, I_m and W_p ($= V_p + V_b$) can be considered to be primary, because they are determined only by the active channel properties which are intrinsic. Other dc parameters, such as I_0 and V_{kf}, are secondary, since they are affected by extrinsic elements outside the gate channel region. The basic channel parameters can be determined only from the *primary* dc parameters, if any one of the three basic parameters for the device under evaluation is known. This is a characteristic of case I.

2.3 Determination of basic channel parameters: Case II

In this case, none of the three basic channel parameters is known. For the determination of these parameters, the *secondary* dc parameters play the major role and the primary dc parameters remain auxiliary. There are two ways to determine the basic channel parameters in this category.

The first method is based on parameter I_0. Rearranging (8) and (12) yields

$$I_s \approx \frac{\sqrt{V_p + V_b + V_c}}{R_s}\left[1 \mp \sqrt{1 - \frac{2I_0R_s}{\sqrt{V_p + V_b + V_c} - 1}}\right]. \tag{18}$$

After knowing I_s, N and a can be determined from (3) and (4), respectively, as follows:

$$N = \frac{1}{V_p + V_b}\left[\frac{12I_s}{Z}\right]^2 \quad (10^{16}\ \text{cm}^{-3}) \tag{19}$$

and

$$a = 0.031\ (V_p + V_b)\frac{Z}{I_s} \quad (\mu\text{m}). \tag{20}$$

Now (17) can be used with (5) to obtain L as

$$L = 4.27\ (V_p + V_b)\left[1 - \frac{I_m}{I_s}\right]^2 \quad (\mu\text{m}). \tag{21}$$

The second method is to utilize parameter V_{kf}. Rewriting (14) yields

$$\beta \approx 1 - \sqrt{\frac{V_{kf} - I_f(R_s + R_d) - V_c}{V_p + V_b}}. \tag{22}$$

After knowing the β value, N and a can be determined by (19) and (20), respectively, provided that $I_s = I_m/\beta$. The L value can be directly determined from (14) and (17) as

$$L = 4.27\,[V_{kf} - I_f(R_s + R_d) - V_c] \quad (\mu\text{m}). \tag{23}$$

The first method demands the known values of Z, V_p, V_b, V_c, I_o, I_m, and R_s, whereas the second method requires Z, V_p, V_b, V_c, V_{kf}, I_f, R_s, and R_d already known. In the computation process of determining N, a, and L, the subtraction of two major terms is included in both cases. Therefore, chances of introducing an intolerable error are inevitable. Thus, taking only a single method is not advisable. The results obtained from one method have to be checked with the other method. The simplified relationship given in (7) could be conveniently used as a guide to examination and adjustment. Expressions (8) through (11) for I_o could also be applied for an additional checking of the determined values of N, a, and L, in comparison with the directly measured value of I_o. Some adjustments on temporarily determined values of the parameters are often necessary to reach their most probable values.

III. MEASUREMENTS OF DC PARAMETERS

As previously mentioned, a transistor curve tracer is used as the test instrument in this paper. A good calibration of the measuring system is essential. Not only the curve tracer but also the test fixture must be taken into consideration. For example, lead resistances may introduce an intolerable measuring error in large-size devices. An excessive leakage current may mislead the determination of junction parameters. Instability and/or relatively low-frequency oscillation, often taking place in a high-performance device, are an annoying phenomena and require a special skill to suppress.

In the following sections, measuring methods for the dc parameters of a GaAs MESFET are described. Although some methods have been known or are easily derived from known methods, they are included with brief descriptions for completeness. The ideality parameter of a gate junction, n, and the open channel resistance, R_o, are needed neither for determination of the basic channel parameters nor for prediction of the microwave performance parameters. Nevertheless, they are secondarily obtained in the course of determination of the primary parameters. As they may be relevant to a further study of the device, their determination is also described.

3.1 Determination of gate barrier built-in voltage and ideality parameter

As is well known,[6] the forward current density, J, of a Schottky barrier junction for $V > 3kT/q$ is approximately written as

$$J = A^*T^2 \exp\left[-\frac{qV_b}{kT}\right]\exp\left[\frac{qV}{nkT}\right], \tag{24}$$

where A^* is the effective Richardson constant, T is the junction temperature in °K, k is the Boltzmann constant, n is the ideality parameter, and V is the forward bias voltage.

The extrapolated value of current density to zero bias gives the saturation current density, J_s. The barrier built-in voltage is then obtained from

$$V_b = \frac{kT}{q} \ln\left[\frac{A^* T^2}{J_s}\right]. \tag{25}$$

The ideality parameter is given by

$$n = \frac{q}{kT} \frac{\partial V}{\partial(\ln J)}. \tag{26}$$

Figure 1 is a multi-exposed photograph of the forward I-V characteristic of a gate junction at room temperature. As described in the caption, each curve corresponds to a current range in a decimal step for several orders of magnitude. In the highest current range, the gate was against three different connections, i.e., source and drain combined, source alone, and drain alone, in order to differentiate R_g, R_s, and R_d from each other later.

The I-V characteristic given in Fig. 1 is plotted as shown in Fig. 2. At high values of the gate bias, V_g, the gate current, I_g, tends to saturate due to the series resistance effect. At low values of V_g, I_g is often disturbed by a leakage current component around the gate

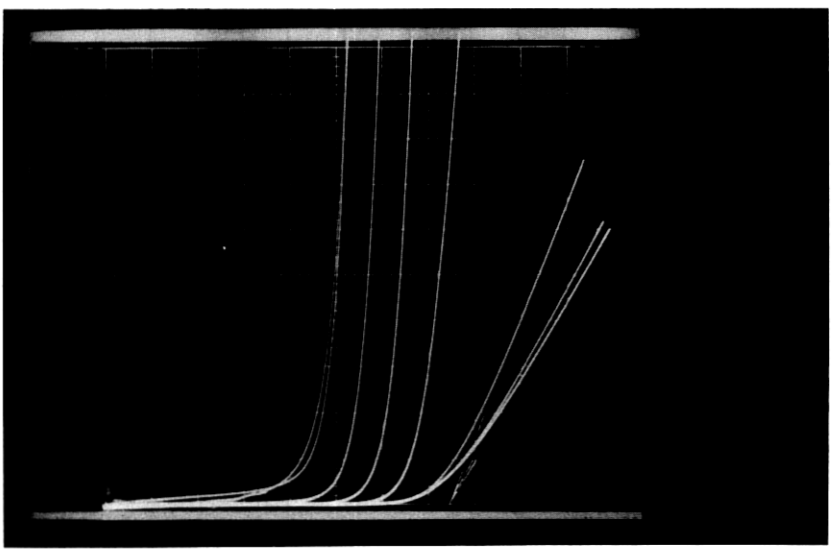

Fig. 1—A multi-exposed photograph of the forward I-V characteristic of a gate junction at room temperature. Each curve corresponds to a current range of decimal step. In the highest current range, three different ground connections are taken against the gate. They are the source and drain connected together, source alone, and drain alone. For all lower current ranges, the drain is connected to the source. The horizontal scale is in units of 0.1 V/div. The vertical scales are, left to right, 1 μA/div, 10 μA/div, 100 μA/div, 1 mA/div, 10 mA/div (source and drain together), 10 mA/div (source only), and 10 mA/div (drain only).

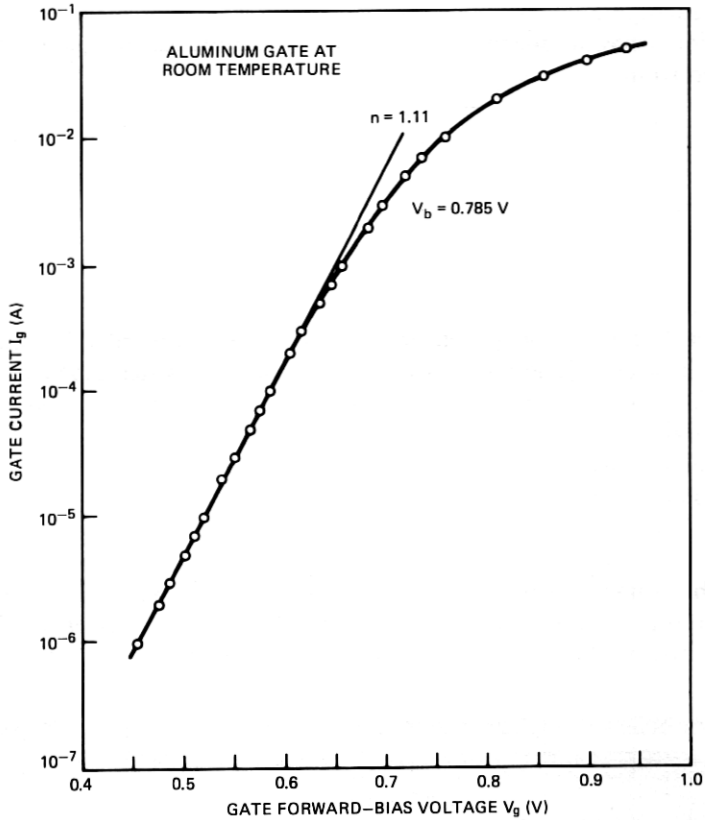

Fig. 2—The forward *I-V* characteristic of an aluminum gate diode at room temperature. The slope and the location of its linear portion on a semi-log paper give the ideality parameter, n, and the gate built-in voltage, V_b, respectively.

periphery or with the package. In the middle range where the log I_g vs V_g characteristic is linear, two gate biases, $V_{g(m)}$ and $V_{g(m-1)}$ in V, can be chosen corresponding to $I_g = 10^m$ and $I_g = 10^{m-1}$ in A, respectively. Usually, m takes a negative value.

If the effective mass of electrons in n-GaAs were taken into account, the effective Richardson constant would be 8.7 A/cm^2/°K at room temperature.[7] Expression (25) for V_b can then be reduced to the following practical form at room temperature:

$$V_b = 0.768 - 0.06 \log J_s \quad \text{(V)}, \tag{27}$$

in which

$$J_s = \frac{10^y}{L_g Z} \quad (10^{-7}\ \text{A/cm}^2) \tag{28}$$

$$y = 12 + m - \frac{1}{1 - \frac{V_{g(m-1)}}{V_{g(m)}}} \tag{29}$$

and L_g is in units of μm and Z is in mm. A formula to be used for deriving n is deduced from (26) as

$$n = 16.8[V_{g(m)} - V_{g(m-1)}]. \tag{30}$$

3.2 Determination of pinch-off voltage, active channel resistance, and parasitic series resistances

Figure 3 shows the drain I-V characteristics in the so-called linear region. The characteristics were taken with the lowest scale of V_{ds} on the curve tracer, in which V_{ds} was the drain-source bias voltage. Each characteristic corresponds to a gate-source bias voltage, V_{gs}. The drain current, I_d, at $V_{ds} = 0.05$ V is then plotted as a function of V_{gs} as shown in Fig. 4. The terminal pinch-off voltage, V_p, can *temporarily* be determined by an extrapolation of the plot to the abscissa.

The current shown in Fig. 4 can now be converted into the resistance value as $R_{ds} = I_d/V_{ds}$. Such a resistance for $V_{ds} = 0.05$ V is shown in Fig. 5 as a function of V_p, V_b, and V_{gs}, in the same manner as used in Ref. 8, as compounded in parameter X defined as

$$X = \frac{1}{1 - \sqrt{\frac{V_b - V_{gs}}{V_b + V_p}}}. \tag{31}$$

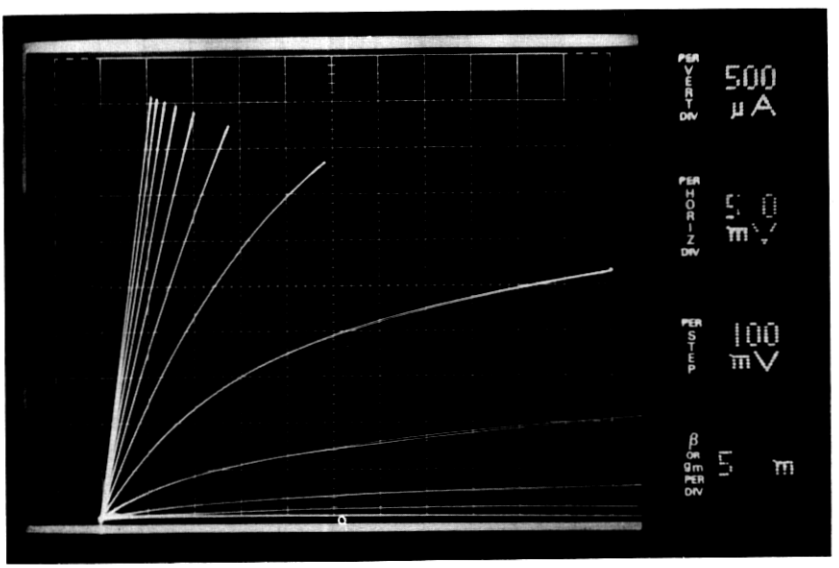

Fig. 3—An expanded view of the drain I-V characteristics in the so-called linear region near the origin on gate-bias offset mode (+0.4 V in this case).

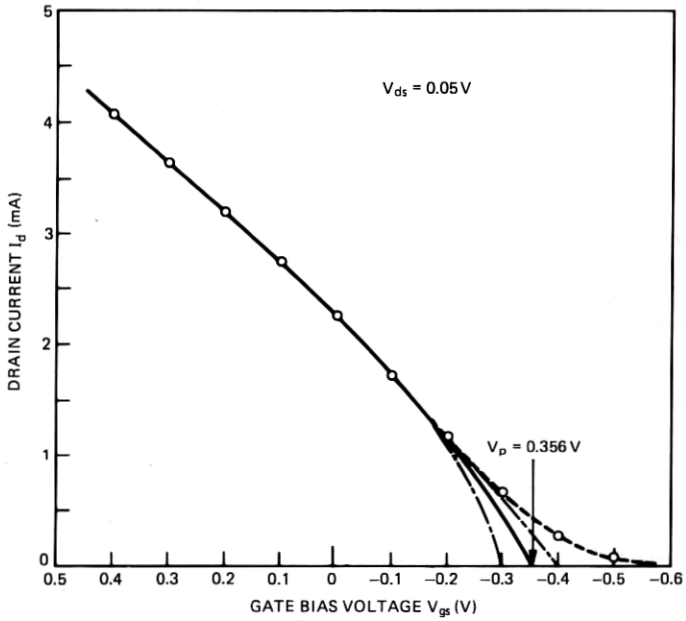

Fig. 4—Drain current as a function of gate bias voltage in both forward and reverse directions at a drain-source bias voltage, V_{ds}, of 0.05 V. An appropriate extrapolation of this curve to the abscissa gives the external (or terminal) pinch-off voltage, V_p. A misjudgment in the determination of V_p, as shown by the dash-dotted line, will cause a problem in the next step.

This plot should be a straight line. However, the plot may deviate from the line either upward or downward as X increases, as indicated by dashed lines in Fig. 5. Such a deviation depends upon the *temporarily* determined value of V_p. If the plot significantly departed from the straight line, the previously determined V_p had to be re-examined. Usually, a slight adjustment on the V_p value easily solves this problem and V_p is *finally* determined.

Such a way of determining V_p seems to be much more complicated and tedious than the conventional method. Usually, V_p is simply estimated from V_{gs} corresponding to the bottom line of the drain I-V characteristics. Indeed, the conventional method may not bring too much error in the determination of V_p in the case of thick active channels, i.e., devices with high pinch-off voltages. However, in devices with thin active channels, especially on buffer layers, the error may reach as high as 100 percent with the conventional method, as will be seen in Fig. 6. Therefore, the present method has been developed.

In Fig. 5, the linear extrapolation of the plot to the ordinate gives the value of $(R_s + R_d)$. The slope of the line is designated as R_o. The

parameter R_oX represents the effective value of active channel resistance at a given V_{gs}.

As was mentioned previously, the forward gate current value is affected by a combination of series resistances at high current levels. Therefore, the slope of the I_g-V_g characteristic, measured at a current density of around 10^4 A/cm^2, gives an estimate of series resistance values. By measuring the gate current in three different ground connections, i.e., source and drain combined, source only, and drain only, three resistance values can be obtained. The differences between the last two values yields $(R_s - R_d)$. Since $(R_s + R_d)$ has been known, R_s and R_d are now readily separated. The gate series resistance R_g can be

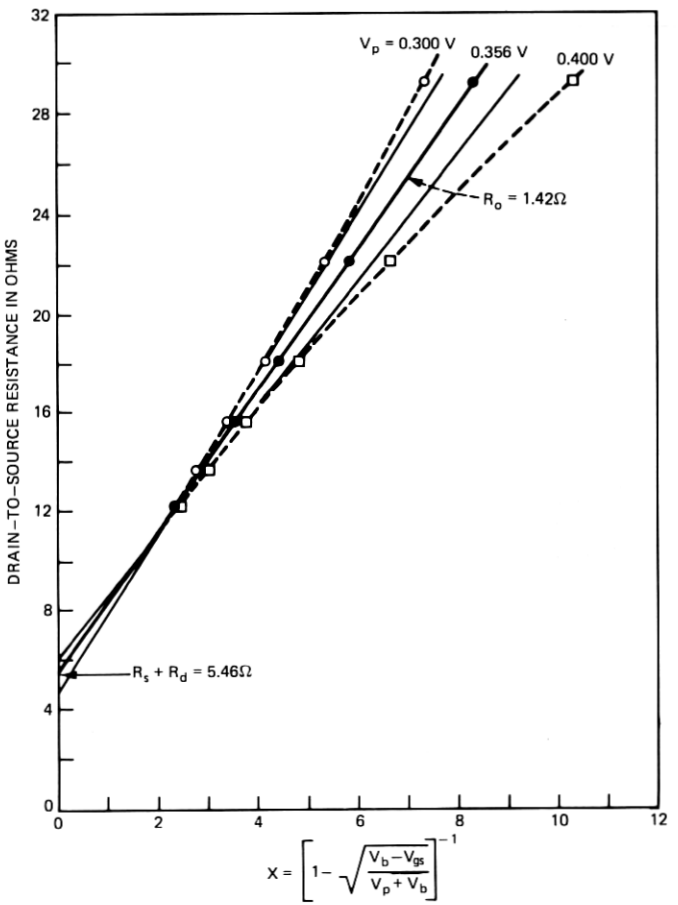

Fig. 5—Determination of the open channel resistance, R_o, and parasitic series resistances, R_s and R_d. The proper selection of V_p value in Fig. 4 (i.e., V_p = 0.356 V in this case) is essential for this determination, as illustrated in two wrong cases (V_p = 0.300 V and 0.400 V).

deduced from the first resistance value by subtracting the contribution of the paralleled R_s and R_d from the resultant.

3.3 Determination of specific voltages and currents

Figure 6 is a typical photograph of the drain I-V characteristics for negative gate potentials, taken with the nonoffset gate-bias mode of the curve tracer. In contrast with Fig. 6, Fig. 7 is an unconventional photograph of the drain characteristics of the same device when driven in the forward gate bias with the offset mode. As the positive value of gate offset is increased, the drain current increases. Beyond a certain value of the offset, V_f, however, the drain current no longer increases. Figure 7 shows such a state of offsetting.

The knee voltage of a drain I-V characteristic could be defined as the intercepting point between the extensions of two linear regions of the characteristic. The knee voltage of the I-V curve for V_f is denoted by V_{kf} as shown in Fig. 7. Also, the knee voltage for the zero-gate-bias curve is by V_{ko} as shown in Fig. 6. Total drain currents, I_f and I_{do}, for V_f and null gate bias, respectively, are measured at the corresponding knee voltages, V_{kf} and V_{ko}. Leakage current components, I_{pf} and I_{po}, are also measured at V_{kf} and V_{ko}, respectively, both for $V_{gs} = -V_p$. The maximum channel current, I_m, and zero-gate-bias channel current, I_o, are then evaluated as $I_f - I_{pf}$ and $I_{do} - I_{po}$, respectively.

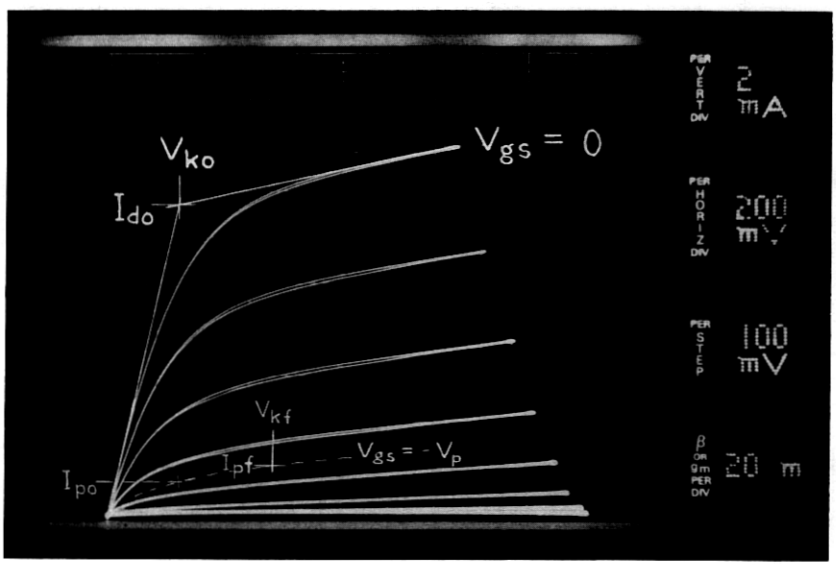

Fig. 6—A conventional drain I-V characteristics with nonoffset gate-bias mode as usual.

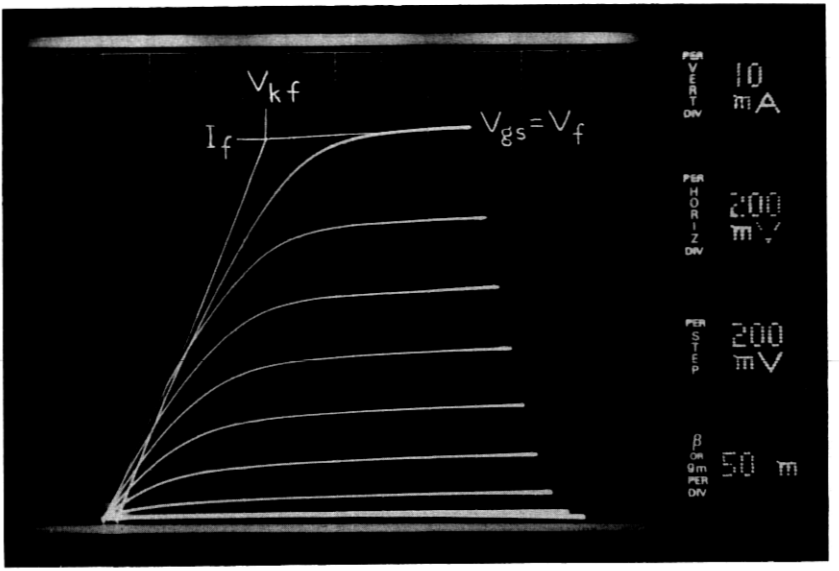

Fig. 7—A special drain I-V characteristics with a forward gate-bias offsetting of V_f. This is a critical value beyond which no increase in the drain current is observed.

3.4 Determination of transconductance

As is well known, the magnitude of the transconductance of a good device can be assumed to remain constant up to nearly the cutoff frequency. Therefore, the so-called dc transconductance can be considered a first-order approximation of the amplitude of microwave transconductance.

The following method of measuring g'_m and evaluating g_m is conventional. In the drain I-V characteristics, an increment of drain current, ΔI_d, between two adjacent curves for $V_{gs} = V_1$ and $V_{gs} = V_2$ at a given V_{ds} yields an average transconductance as

$$g'_m = \left| \frac{\Delta I_d}{V_2 - V_1} \right|. \tag{32}$$

However, this value is a result of degradation due to R_s. The intrinsic value of the small-signal transconductance at the bias points, $V_{ds} = V_{ds}$ and $V_{gs} = (V_1 + V_2)/2$, can thus be derived as

$$g_m \approx \frac{g'_m}{1 - g'_m R_s}. \tag{33}$$

IV. EXAMINATIONS OF NEW TECHNIQUE

4.1 Sample devices

To present the practical values of measured dc parameters and hence to demonstrate the new technique for determining the basic

channel parameters, 11 GaAs MESFETs of various designs were chosen, as shown in Table I. The first five devices (A through E) were originally designed for high-power use[9] and the others (F through K) were for low-noise applications.[10]

All devices had a total device width of 0.5 mm, except for device E which had 1 mm. The distance between the source and drain electrodes was nominally 6 μm for devices A through E and 3 μm for devices F through K. The nominal gate length was 2.0 to 2.5 μm for devices A to D, 1.0 to 1.5 μm for device E, and 0.8 μm for devices F to K. The physical length of the gate electrode, however, was not necessarily equal to the effective gate length because the latter was subject to the shape of a gate junction.

All the sample devices had a multi-layer structure consisting of an undoped n-GaAs film 2 to 3 μm thick as the buffer, an n-GaAs channel, and n^+-GaAs layer, except for devices J and K. All the layers were grown sequentially on a semi-insulating GaAs substrate in an $AsCl_3$/Ga/H_2 CVD system.[11] After removing the n^+-GaAs layer and part of n-GaAs in the gate region, aluminum approximately 0.7 μm thick was deposited as the Schottky-gate metal. The ohmic contacts were formed with a 12 percent Ge/Au-Ag-Au system approximately 0.25 μm thick, alloyed at nearly 500°C. The final metallization was completed with a Ti-Pt-Au system 0.9 to 1.4 μm thick.

4.2 Results of measurements

First, dc parameters n, V_b, V_p, W_p, V_{kf}, V_f, I_f, I_{pf}, I_m, V_{ko}, I_{do}, I_{po}, I_o, R_o, R_s, R_d, R_g and g'_m were obtained in accordance with the measuring technique described in Section III. The measured values of these parameters are shown in Table I. Note that g'_m is an average value taken at approximately I_o.

Second, basic channel parameters L and N were deduced from each of the two methods described in Section 2.3. In the application of (18), (22), and (23), V_c was assumed to be zero for devices A to E and to be a single value of 0.17 V for devices F to K. The two deduced values for each of L and N were then averaged to obtain the most probable value. Using this mean value of N in (15), the most probable value of a was determined. All values mentioned here are shown in Table II.

4.3 Comparison of calculated and measured results

By inserting the determined values of N, a, and L into (4), (6), and (5), I_m was calculated. The calculated value of I_m was then compared with the measured value as shown in Table III. By adopting the measured value of V_b and R_s in (10) and (11), respectively, I_o was also calculated using (9), (4), and (8). The calculated I_o was compared with the measured value, again as shown in Table III. The comparison has shown excellent agreement between the calculated and measured

Table I—Measured values of dc parameters

Parameter		Device										
Symbol	Units	A	B	C	D	E	F	G	H	I	J	K
Z	mm	0.5	0.5	0.5	0.5	1.0	0.5	0.5	0.5	0.5	0.5	0.5
z	mm	0.5	0.25	0.25	0.5	0.25	0.25	0.25	0.25	0.25	0.25	0.25
n		1.09	1.07	1.26	1.34	1.26	1.46	1.12	1.23	1.23	1.34	1.26
V_b	V	0.72	0.73	0.76	0.79	0.74	0.74	0.78	0.76	0.74	0.76	0.76
V_p	V	5.84	6.07	3.51	1.16	4.88	1.15	0.51	0.34	0.54	0.52	0.36
W_p	V	6.56	6.80	4.27	1.95	5.62	1.89	1.29	1.10	1.28	1.28	1.12
V_{kf}	V	1.95	1.95	2.10	1.55	1.85	0.75	0.59	0.68	0.77	1.08	0.83
V_f	V	1.49	1.34	1.80	1.49	1.62	1.39	0.97	0.96	1.12	1.30	1.14
I_f	mA	176	196	179	136	400	83.0	86.0	82.0	107	94.0	87.5
I_{pf}	mA	1	1	2	2	5	4.0	1.5	1.5	4	3.0	3.0
I_m	mA	175	195	177	134	395	79.0	84.5	80.5	103	91.0	84.5
V_{ko}	V	1.5	1.5	1.4	0.7	1.4	0.55	0.3	0.3	0.4	0.3	0.3
I_{do}	mA	122	134	104	39.5	257	32.0	20	13	24.0	19.5	14.5
I_{po}	mA	0	1	1	1.5	3	2.7	1	1	2.5	2	2
I_o	mA	122	133	103	38.0	254	29.3	19	12	21.5	17.5	12.5
R_o	Ω	4.1	3.0	2.9	3.4	1.2	4.0	2.9	2.9	2.5	2.7	3.0
R_s	Ω	4.8	3.7	4.5	5.2	1.8	2.7	1.5	2.3	2.3	3.8	2.9
R_d	Ω	2.4	3.6	4.0	2.8	1.7	2.7	1.9	2.4	2.3	4.8	3.4
R_g	Ω	3.8	1.7	1.7	4.5	4.4	13.7	3.8	3.7	4.0	4.5	3.8
g'_m	m℧	28	32	28	53	72	30	45	51	52	45	48

Table II—Determination of the most probable values of active channel carrier concentration and thickness and effective gate length

Parameter			Device										
Equations Used	Symbol	Units	A	B	C	D	E	F	G	H	I	J	K
	V_c	V	0	0	0	0	0	0.17	0.17	0.17	0.17	0.17	0.17
(18, 19)	N	10^{16} cm^{-3}	6.01	5.98	11.19	21.16	7.96	3.52	6.34	7.75	9.84	7.59	7.91
(18, 21)	L	μm	3.07	2.06	2.71	2.08	2.04	0.568	0.466	0.537	0.502	0.491	0.486
(21, 5, 19)	N	10^{16} cm^{-3}	5.86	6.15	10.58	20.13	7.78	3.51	6.78	7.76	9.83	7.23	8.31
(23)	L	μm	2.91	2.22	2.47	1.97	1.92	0.563	0.545	0.532	0.503	0.436	0.538
(averaged)	N	10^{16} cm^{-3}	5.94	6.07	10.89	20.65	7.87	3.52	6.56	7.76	9.84	7.41	8.11
(averaged)	L	μm	2.99	2.14	2.59	2.03	1.98	0.566	0.508	0.534	0.502	0.463	0.512
(15)	a	μm	0.391	0.394	0.233	0.114	0.314	0.273	0.165	0.140	0.134	0.155	0.138

Table III—Calculated values of the maximum channel current and zero-gate-bias channel current and their comparison with measured values

Parameter			Device										
Equations used	Symbol	Units	A	B	C	D	E	F	G	H	I	J	K
(4, 5, 6)	I_m	mA	175	195	177	134	395	79.0	84.4	80.6	103	91.0	84.4
(4, 8, 9, 10, 11)	I_o	mA	118	133	99.0	36.2	272	31.0	18.5	11.0	23.1	18.4	12.1
I_m (cal)/I_m (meas)			1.000	0.999	1.000	1.000	1.000	1.000	0.999	1.001	1.000	1.000	0.999
I_o (cal)/I_o (meas)			0.965	1.002	0.971	0.953	1.069	1.058	0.973	0.916	1.076	1.054	0.966

values in both cases. Note that the equations applied to calculate I_m and I_o had not been used to determine L, a, and N in Section 4.2.

The 11 devices used in this experiment were from 11 different slices. The free carrier concentration of each slice was evaluated by a doping profiler.[12] It has been recognized that this particular profiler gives an N-value 5 to 40 percent higher than the true value of N.[13] Also, a standard deviation of ± 3 percent in the doping across a wafer has been known for these slices.[11] Under such circumstances, the evaluated value of N for each device was compared with an uncorrected, representative N value obtained for the corresponding slice. The results shown in Table IV seem to be very reasonable. A consistent pattern of difference between the two N values is seen there, as expected from the above observation.

V. ANALYSES OF EXPERIMENTAL RESULTS

5.1 Schottky-barrier built-in voltage

The built-in voltage of an aluminum Schottky-barrier gate junction at room temperature has been expressed in an analytical form as a function of N in n-GaAs[1] as follows:

$$V_b = 0.706 + 0.06 \log N \quad \text{(V)}, \tag{34}$$

where N is in units of 10^{16} cm^{-3}. This expression is compared with the measured value of V_b for all devices used, as shown in Fig. 8. This comparison indicates that (34) can be used for aluminum gates on n-GaAs at room temperature.

5.2 Transconductance

The small-signal transconductance of a GaAs MESFET has been described by the theoretical expression[5]

$$g_m = \frac{I_s}{2W_p\left[1 - \dfrac{I_d}{I_s}\right]}, \tag{35}$$

where I_d is the dc drain bias current. Since g'_m was measured approximately at I_o, the theoretical value of g_m was also calculated for $I_d = I_o$ in (35). This calculated value was then compared with the measured value obtained using (33). This comparison led to a conclusion that the measured value of g_m would agree well with the predicted value if the latter were calculated by

$$g_m \approx \frac{0.9\, I_s}{2(V_p + V_b)\left[1 - \dfrac{I_c}{I_s}\right]}, \tag{36}$$

Table IV—Comparison of the most probable value of free carrier concentration in the active channel of an individual device with an uncorrected value of doping in the epitaxial layer of the corresponding slice

Parameter		Device										
Symbol	Units	A	B	C	D	E	F	G	H	I	J	K
N (slice) uncorrected	10^{16} cm^{-3}	6.7	7.4	14.2	24.6	8.8	4.1	7.1	9.0	10.4	8.1	11.2
N (slice)/N(device) uncor. most prob.		1.13	1.22	1.30	1.20	1.12	1.16	1.08	1.16	1.06	1.09	1.38

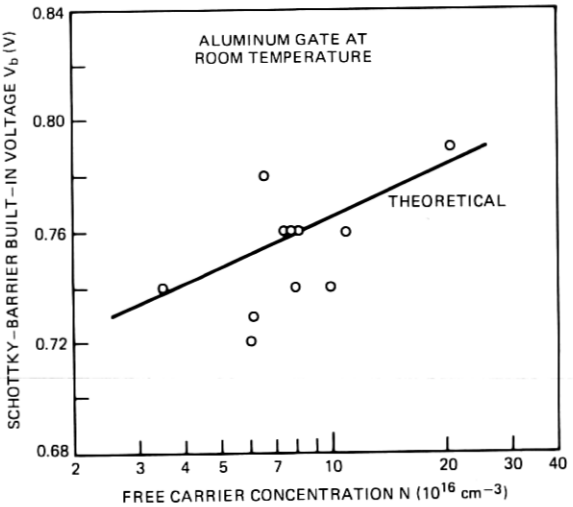

Fig. 8—Comparison of the measured values of gate built-in voltage for aluminum Schottky-barrier gates at room temperature, with a theoretical expression as a function of free carrier concentration in n-GaAs.

where I_c was the channel current, as shown in Table V.

5.3 Ohmic contacts and series channel resistance

The parasitic series resistance, R_s or R_d, consists of the ohmic contact resistance, R_{co}, and series channel resistance, R_{ch}, between the two concerned electrodes. These component resistances are now separately expressed. The expression for R_{co} given by Berger[14] and Murrmann and Widmann[15] can be simplified, as already shown by Macksey and Adams[16] as

$$R_{co} = \frac{1}{Z}\sqrt{\frac{R_c\rho_1}{a_1}}\coth\sqrt{\frac{\rho_1 L_c^2}{R_c a_1}} \approx \frac{1}{Z}\sqrt{\frac{R_c\rho_1}{a_1}}. \tag{37}$$

The series channel resistance can be further divided into two components which represent two individual parts of different structures in the space between the gate and one ohmic contacts.
Thus,

$$R_{ch} \approx R_2 + R_3, \tag{38}$$

where

$$R_2 = \frac{\rho_2 L_2}{Z a_2} \tag{39}$$

and

$$R_3 = \frac{\rho_3 L_3}{Z a_3}. \tag{40}$$

Table V—Measured and predicted values of transconductance at zero-gate-bias channel current

Parameter	Device										
g_m @ I_o	A	B	C	D	E	F	G	H	I	J	K
Measured (m℧)	32	36	46	69	83	33	48	58	59	54	56
Predicted (m℧)	33.6	35.2	47.4	71.2	81.9	35.1	50.0	55.4	60.9	52.1	56.2

In the above expressions, $a_{i=1,2,3}$, $\rho_{i=1,2,3}$ and $L_{i=2,3}$ are, respectively, the thickness, specific resistivity, and length of the GaAs epitaxial film at the corresponding place $i = 1$, 2 or 3, L_c is the length of the contacting metal electrode, and R_c is the specific contact resistance.

Parameters ρ and R_c are both functions of N. Using the experimental data taken by Matino on epitaxial n-GaAs films,[17] the doping dependence of ρ can be written in an analytical form

$$\rho \approx 0.11\, N^{-0.82} \quad (\Omega\text{-cm}) \tag{41}$$

in an N range of 10^{-1} to $10^3 \times 10^{16}$ cm^{-3}. Based on the so-called Shockley method,[8] R_c was statistically investigated using monitor areas provided within the same slices as those fabricated for either high-power[9] or low-noise use.[10] An empirical expression for R_c was then found to be

$$R_c \approx 4\, N^{-0.5} \quad (10^{-5}\ \Omega\text{-cm}^2) \tag{42}$$

for N values in the range of 3 to $10^3 \times 10^{16}$ cm^{-3}. This expression differs from that given by Heime et al.,[18] which is

$$R_c \approx 8\, N^{-1} \quad (10^{-5}\ \Omega\text{-cm}^2). \tag{43}$$

However, both expressions give close values of R_c for N in the vicinity of the mid-10^{16} cm^{-3} range. As the N value increases, the difference in R_c between the two expressions becomes recognizable. This would give rise to the case of ohmic contacts formed on n$^+$-GaAs layers. An estimate by (43) would result in too-optimistic prediction of R_c.

Substitution of (41) and (42) into (37), (39), and (40) yields practical expressions for R_{co}, R_2, and R_3 as follows:

$$R_{co} \approx \frac{2.1}{Z a_1^{0.5} N_1^{0.66}} \quad (\Omega) \tag{44}$$

$$R_2 \approx \frac{1.1\, L_2}{Z a_2 N_2^{0.82}} \quad (\Omega) \tag{45}$$

and

$$R_3 \approx \frac{1.1\, L_3}{Z a_3 N_3^{0.82}} \quad (\Omega). \tag{46}$$

For the 11 sample devices with reasonable assumptions on N_1, a_1, L_2, N_2, a_2, L_3,, N_3, and a_3, component resistances R_{co}, R_2, and R_3 were calculated using (44), (45), and (46), respectively. The predicted

value of R_s (or R_d) was thus obtained as the sum of these resistances. The average of the measured values of R_s and R_d for each device was then compared with the predicted value, as shown in Table VI. They were in good agreement.

5.4 Gate series resistance

Since the input signal applied to the feeding end of the gate travels along the gate metallization to the other end, the gate must be considered as a distributed network. The effective value of the gate metallization resistance in a lumped equivalent circuit is, therefore, different from the dc value measured from one end to the other. As theoretically analyzed by Wolf,[19] this effective value, R_g, is one-third of the end-to-end dc resistance as a first-order approximation. Thus,

$$R_g \approx \frac{\rho_g z^2}{3L_g h Z}, \tag{47}$$

where ρ_g is the specific resistivity, L_g is the mean length, h is the mean height, and z is the unit width of the gate metallization.

By substituting the nominal values of Z, z, L_g and h into (47) in conjunction with the measured value of R_g, ρ_g was evaluated as shown in Table VII. The range from 3.8 to 5.7 $\times$ 10^{-6} Ω-cm gives a mean value of 5.0 $\times$ 10^{-6} Ω-cm. Although this value is higher than a bulk aluminum resistivity of 2.8 $\times$ 10^{-6} Ω-cm, it seems to be very reasonable for such a fine, thin, and scaly structure of gate metallization. Based on this finding, a practical expression for R_g can be given by

$$R_g \approx \frac{17z^2}{L_g h Z} \quad (\Omega), \tag{48}$$

where Z and z are in units of mm and L_g and h are in μm.

It may be noted that annealing of a device sometimes results in an improvement in the effective value of ρ_g. The above measured values were obtained without additional heat treatment.

5.5 Open channel resistance

The open channel resistance mentioned in Section III can be expressed as

$$R_o = \frac{L}{q\mu_0 N a Z}, \tag{49}$$

where μ_0 is the low-field mobility of electrons.[8] Thus, μ_0 of an individual device can be obtained from the measured value of R_o in conjunction with Z, L, a, and N, which have already been determined.

On the other hand, μ_0 is related to ρ in the form

$$\mu_0 = \frac{1}{qN\rho}. \tag{50}$$

Table VI—Predicted values of parasitic source (or drain) series resistance and its component resistances in comparison with measured value

Parameter		Device										
Symbol	Units	A	B	C	D	E	F	G	H	I	J	K
Z	mm	0.5	0.5	0.5	0.5	1.0	0.5	0.5	0.5	0.5	0.5	0.5
N_1	10^{16} cm^{-3}	100	100	50	100	100	100	100	100	100	7.4	8.1
a_1	μm	0.15	0.15	0.15	0.15	0.15	0.15	0.15	0.15	0.15	0.35	0.45
L_2	μm	2.1	2.1	2.1	2.1	2.5	0.85	0.75	0.85	0.85	0.75	0.75
N_2	10^{16} cm^{-3}	5.9	6.1	10.9	20.7	7.9	100	100	100	100	7.4	8.1
a_2	μm	0.35	0.35	0.2	0.1	0.35	0.1	0.1	0.1	0.1	0.25	0.35
L_3	μm	0	0	0	0	0	0.4	0.3	0.4	0.4	0.3	0.3
N_3	10^{16} cm^{-3}	—	—	—	—	—	3.5	6.6	7.8	9.8	7.4	8.1
a_3	μm	—	—	—	—	—	0.273	0.165	0.140	0.134	0.155	0.138
R_{co}	Ω	0.52	0.52	0.82	0.52	0.26	0.52	0.52	0.52	0.52	1.89	1.57
R_2	Ω	3.07	3.01	3.26	3.86	1.45	0.68	0.59	0.68	0.68	1.28	0.85
R_3	Ω	0	0	0	0	0	1.15	0.86	1.17	1.00	1.13	0.86
Predicted R_s, R_d	Ω	3.59	3.53	4.08	4.38	1.71	2.35	1.97	2.37	2.20	4.30	3.28
Measured $(R_s + R_d)/2$	Ω	3.6	3.65	4.25	4.5	1.75	2.7	1.7	2.35	2.3	4.3	3.15

Table VII—Determination of the effective resistivity for aluminum gate metallization

Parameter		Device										
Symbol	Units	A	B	C	D	E	F	G	H	I	J	K
Z	mm	0.5	0.5	0.5	0.5	1.0	0.5	0.5	0.5	0.5	0.5	0.5
z	mm	0.5	0.25	0.25	0.5	0.25	0.25	0.25	0.25	0.25	0.25	0.25
L_R	μm	2.5	2.0	2.0	2.0	1.2	0.8	0.8	0.8	0.8	0.8	0.8
h	μm	0.7	0.7	0.7	0.7	0.2	0.2	0.65	0.65	0.65	0.65	0.65
R_R	Ω	3.8	1.7	1.7	4.5	4.4	13.7	3.8	3.7	4.0	4.5	3.8
ρ_R	10^{-6} Ω-cm	4.0	5.7	5.7	3.8	5.1	5.3	4.9	4.8	5.0	5.6	4.9

Substituting (41) into (50) yields μ_0 as a function of N

$$\mu_0 \approx 5.7\, N^{-0.18} \quad (10^3 \text{cm}^2/\text{V-sec}). \tag{51}$$

The μ_0 value deduced from the measured value of R_o and that predicted by (51) are shown in Table VIII for all the sample devices. The evaluation of the latter value was based on the average value of N shown in Table II. In the high-power devices, these two values of μ_0 were close enough to confirm Matino's results[17] and to support the use of (41) and (51). In the low-noise devices, however, the μ_0 value deduced from R_o appeared to be approximately one-half the predicted value by (51). Such a discrepancy might be caused by a special two-dimensional gate-recess structure of these devices, and/or be due to an increased influence of the transition layer as the active layer was thinned, this transition layer being between the active and buffer layers. This is subject to further investigation.

As shown in Table VIII, the μ_0 value deduced from the measured value of R_o using (49) differs from one device to the other in some degree. In accordance with the two-piece approximation of the v-E characteristic, however, μ_0 is assumed to be constant by definition and is equal to v_s/E_c. Substituting the aforementioned best-fit values of v_s and E_c into this yields a fixed value of 4.8×10^3 cm^2/V-sec for μ_0, which is independent of N. This μ_0 value is much greater than that deduced from R_o by (49) and that calculated by (51) as a function of N in the normal range. On the contrary, the fixed values of v_s and E_c have been satisfactory to evaluate I_m for a wide range of N, as seen in the previous sections. Such a conflicting situation must be reconciled. This is also subject to further study. Nevertheless, the following can be applied in practice, for the time being. The fixed values of v_s and E_c are appropriate for the evaluation of I_m for all devices. The μ_0 value provided by (51) is adequate in (49) to calculate R_o for devices with plane gates. However, a suitable correction factor is necessary for μ_0 given by (51) to make μ_0 effective for nonplane gate devices. For example, this factor was 0.5 for the low-noise devices used as samples.

Table VIII—Comparison between the low-field electron mobility value deduced from the measured value of open channel resistance by (49) and that predicted from the most probable value of free-carrier concentration in the active channel by (51)

Parameter	Device										
μ_0 in 10^3 cm^2/V-sec	A	B	C	D	E	F	G	H	I	J	K
Calculated by (49)	3.9	3.7	4.4	3.2	4.2	1.8	2.0	2.1	1.9	1.9	1.9
Calculated by (51)	4.1	4.1	3.7	3.3	3.9	4.5	4.1	3.9	3.8	4.0	3.9

VI. PREDICTION OF MICROWAVE PERFORMANCE

6.1 Maximum output power

As was previously mentioned, devices A through E were originally designed for high-power use. The maximum available output power, P_{max}, of these devices were measured at 4 GHz in a coaxial system. A double-slug tuner was provided in each of the input and output circuits to obtain the conjugate match. The data taken at a drain bias of 12V are shown in Table IX.

The maximum output power delivered from a GaAs MESFET operating at a drain-source voltage of V_{ds} is approximately given by

$$P_{max} \approx \frac{I_m}{4}(V_{ds} - V_{kf}) \tag{52}$$

if V_{ds} is sufficiently lower than the drain-source breakdown voltage. By substituting the measured values of I_m and V_{kf} into (52), P_{max} was calculated for $V_{ds} = 12$V. Furthermore, P_{max} was predicted using the geometrical and material parameters, shown in Tables II and VI, to calculate I_m and V_{kf}. Both predicted values of P_{max} are shown in Table IX.

As seen in Table IX, there is excellent agreement between the measured and predicted values of P_{max} in devices C, D, and E at this drain bias voltage. However, the measured values of devices A and B were substantially smaller than the predicted values. This discrepancy could be caused by the saturation effect in output power as V_{ds} increased. This problem of power saturation will be discussed in a separate paper. Without power saturation mechanisms, *the maximum output power capability at microwave frequencies can be predicted by dc parameters as well as by device geometrical and material parameters.*

6.2 Minimum noise figure

Devices F through K were originally designed for low-noise amplifiers. The minimum noise figure, F_{min}, of these devices was measured at 5.92 GHz in a coaxial system with double-slug tuners. The measured values are shown in Table X.

Table IX—Predicted and directly measured values of the maximum output power at 4 GHz and 12V drain bias

Parameter	Device				
P_{max} @ 12 volts	A	B	C	D	E
Measured directly (W)	0.40	0.40	0.44	0.36	1.00
Predicted from measured dc para's (W)	0.439	0.491	0.437	0.350	1.001
Predicted from geo. and mat. para's (W)	0.439	0.493	0.440	0.353	1.006

Table X—Predicted and directly measured values of the minimum noise figure at 5.92 GHz

Parameter	Device					
F_{min} @ 5.92 GHz	F	G	H	I	J	K
Measured directly (dB)	2.22	1.51	1.84	1.74	1.75	1.76
Predicted from measured dc para's (dB)	2.21	1.50	1.80	1.73	1.75	1.76
Predicted from geo. and mat. para's (dB)	2.12	1.56	1.79	1.70	1.72	1.80

A simple expression for F_{min} has been derived as

$$F_{min} \approx 10 \log [1 + KfL \sqrt{g_m(R_g + R_s)}] \quad \text{(dB)}, \tag{53}$$

where f is the frequency of interest in GHz and K is the fitting factor.[20] This fitting factor, which represents the channel material properties, ranges from 0.25 to 0.3 in most cases. Substituting (33) into (53) with a typical K-value of 0.27 yields

$$F_{min} \approx 10 \log \left[1 + 0.27 fL \sqrt{\frac{g'_m(R_g + R_s)}{1 - g'_m R_s}} \right] \quad \text{(dB)}. \tag{54}$$

Using the measured values of g'_m, R_g, and R_s, and deduced value of L in (54), F_{min} was calculated for devices F to K. The minimum noise figure was also predicted from the geometrical and material parameters, using the values shown in Tables II, VI, and VII to calculate g_m, R_s, and R_g.

These predicted values are compared with the directly measured value in Table X. The agreement is excellent between them. This supports the idea that *the dc characterization of a low-noise GaAs MESFET makes it possible to predict F_{min} at microwave frequencies with a remarkably high accuracy.* Also, *once the geometrical and material parameters are given for a device, its F_{min} can be calculated as well.* It would be worthwhile to note that, if the operating frequency approaches the cutoff frequency of a device or frequencies where the skin effect on the gate metallization becomes significant, an additional term is required in (54) for an improved accuracy.[20]

VII. SUMMARY OF RELATIONSHIPS

Table XI is a summary of the relationships between the dc and rf performance parameters and the geometrical and material parameters of a GaAs MESFET.

VIII. CONCLUSIONS

This paper complements the recent study of a new model of the GaAs MESFET.[1] A new technique has been introduced in which the basic channel parameters, such as the effective gate length, channel doping, and channel thickness, are determined from the so-called dc

Table XI—Summary of relationships

dc Parameter	Equations	Participating Geometrical and Material Parameters
V_b	(34)	N
W_p	(3)	N, a
V_p	(3, 34)	N, a
I_s	(4)	N, a, Z
β	(6)	N, a, L
I_m	(5, 6, 4) or (7)	N, a, L, Z
R_s, R_d	(44, 45, 46)	$N, N^+, a_1, a_2, a_3, L_2, L_3, Z$
R_g	(48)	Z, z, h, L_g, ρ_g
I_o	(8, 9, 10, 11, 4) or (8, 12, 13, 3, 4)	N, a, L, Z, R_s N, a, Z, R_s, V_c
V_{hf}	(14, 3, 4, 5, 6, 44, 45, 46)	$N, a, L, Z, R_s, R_d, V_c$
Performance Parameter	**Equations**	**Above Parameters plus Bias Parameter**
g_m	(36, 3, 4)	N, a, L, Z, I_c
g'_m	(36, 33, 3, 4, 44, 45, 46)	N, a, L, Z, R_s, I_c
P_{max}	(52, 3, 4, 5, 6, 14, 44, 45, 46)	$N, a, L, Z, R_s, R_d, V_{ds}$
F_{min}	(54, 36, 3, 4, 44, 45, 46, 48)	N, a, L, R_s, R_g, f

parameters. Also, a precise technique developed for measuring the dc parameters was shown. Using 11 sample devices chosen from a wide variety of designs, usefulness of the new techniques was demonstrated.

The determined values of the basic channel parameters for the sample devices were used to calculate their dc parameters, such as the maximum channel current, zero-gate-bias channel current, and transconductance in the simple, analytical expressions recently obtained.[1] Their predicted values were then compared with the measured values in excellent agreement for all devices used. Practical expressions, in terms of device geometrical and material parameters, developed for parasitic resistances were verified in good agreement with measured values on all sample devices.

Using the sample devices, it was demonstrated that the maximum output power and minimum noise figure at microwave frequencies can be predicted by dc parameters as well as by device geometrical and material parameters through simple, analytical expressions. In other words, proper dc characterization of a GaAs MESFET makes it possible to predict the microwave power handling capability and minimum noise property.

Finally, the relationships between the dc and rf performance parameters of a GaAs MESFET and its geometrical and material parameters were summarized with the relevant equations. This summary would be very useful as a handy reference for the design and optimization processes of a GaAs MESFET.

IX. ACKNOWLEDGMENTS

The author is grateful to J. V. DiLorenzo, H. M. Cox, L. A. D'Asaro,

B. S. Hewitt, L. C. Luther, W. C. Niehaus, W. Robertson, P. F. Sciortino, J. A. Seman, and J. R. Velebir for fabricating the sample devices used in this paper. He is also thankful to J. P. Beccone, D. E. Iglesias, F. M. Magalhaes, and W. O. Schlosser for preparing the microwave test equipment used for the output power and noise measurements, and to J. E. Kunzler and L. J. Varnerin for their support of the GaAs MESFET project.

REFERENCES

1. H. Fukui, "Channel Current Limitations in GaAs MESFETS," unpublished work.
2. W. Shockley, "A unipolar 'field-effect' transistor," Proc. IRE, *40* (November 1952), pp. 1365–1376.
3. A. B. Grebene and S. K. Ghandhi, "General Theory for Pinched Operation of the Junction Gate FET," Solid-State Elec., *12* (July 1969), pp. 573–585.
4. R. B. Fair, "Graphical Design and Iterative Analysis of the dc Parameters of GaAs FET's," IEEE Trans. Electron Devices, *ED-21* (June 1974), pp. 357–362.
5. R. A. Pucel, H. A. Haus, and H. Statz, "Signal and Noise Properties of Gallium Arsenide Microwave Field-Effect Transistors," *Advances in Electronics and Electron Physics*, vol. 38, New York: Academic Press, 1975, pp. 195–265.
6. S. M. Sze, *Physics of Semiconductor Devices*, New York: Wiley-Interscience, 1969, p. 393.
7. C. R. Crowell, J. C. Sarace, and S. M. Sze, "Tungsten-Semiconductor Schottky-Barrier Diodes," Trans. Metallurgical Soc. AIME, *233*, (March 1965), pp. 478–481.
8. P. L. Hower, W. W. Hooper, B. R. Cairns, R. D. Fairman, and D. A. Tremere, "The GaAs Field-Effect Transistor," *Semiconductors and Semimetals*, vol. 7, New York: Academic Press, 1971, pp. 147–200.
9. W. C. Niehaus, H. M. Cox, B. S. Hewitt, S. H. Wemple, J. V. DiLorenzo, W. O. Schlosser, and F. M. Magalhaes, "GaAs Power MESFETs," *Gallium Arsenide and Related Compounds (St Louis), 1976*, Conf. Series No. 33b, Bristol and London: The Institute of Physics, 1977, pp. 271–280.
10. B. S. Hewitt, H. M. Cox, H. Fukui, J. V. DiLorenzo, W. O. Schlosser, and D. E. Iglesias, "Low-Noise GaAs MESFETS: Fabrication and Performance," *Gallium Arsenide and Related Compounds (Edinburgh), 1976*, Conf. Series No. 33a, Bristol and London: The Institute of Physics, 1977, pp. 246–254.
11. H. M. Cox and J. V. DiLorenzo, "Characteristics of an $AsCl_3/Ga/H_2$ Two-Bubbler GaAs CVD System for MESFET Applications," *Gallium Arsenide and Related Compounds (St Louis), 1976*, Conf. Series No. 33b, Bristol and London: The Institute of Physics, 1977, pp. 11–22.
12. G. L. Miller, "A Feedback Method for Investigating Carrier Distributions in Semiconductors," IEEE Trans. Electron Devices, *ED-19* (October 1972), pp. 1103–1108.
13. H. M. Cox, private communication.
14. H. H. Berger, "Contact Resistance on Diffused Resistors," 1969 IEEE ISSCC Digest of Technical Papers, February 1969, pp. 160–161.
15. H. Murrmann and D. Widmann, "Current Crowding on Metal Contacts to Planar Devices," 1969 IEEE ISSCC Digest of Technical Papers, February 1969, pp. 162–163.
16. H. Macksey and R. Adams, "Fabrication Processes for GaAs Power FET's," Proc. Fifth Cornell Conf. on Active Semiconductor Devices for Microwave and Integrated Optics, 1975, pp. 255–264.
17. H. Matino, "A Study of GaAs Microwave Semiconductor Devices," Doctoral Dissertation (Japanese), 1972.
18. K. Heime, U. König, E. Kohn, and A. Wortmann, "Very low resistance Ni-AuGe-Ni contacts to n-GaAs," Solid-State Elec. *17* (1974), pp. 835–837.
19. P. Wolf, "Microwave Properties of Schottky-Barrier Field-Effect Transistors," IBM J. Res. Develop., *14* (March 1970), pp. 125–141.
20. H. Fukui, "Optimal Noise Figure of Microwave GaAs MESFETS," unpublished work.